

# Kinematic Calibration of Parallel Mechanisms: A Novel Approach Using Legs Observation

Pierre Renaud, Nicolas Andreff, Philippe Martinet, and Grigore Gogu

**Abstract**—In this paper, a novel approach is proposed for the kinematic calibration of parallel mechanisms with linear actuators at the base. The originality of the approach lies in the observation of the mechanism legs with a camera, without any mechanism modification. The calibration can hence be achieved online, as no calibration device is linked to the end-effector, on any mechanism since no additional proprioceptive sensor installation is necessary. Because of the conditions of leg observability, several camera locations may be needed during the experimentation. The associated calibration method does not however require any accurate knowledge of the successive camera positions. The experimental procedure is therefore easy to perform. The method is developed theoretically in the context of mechanisms with legs linearly actuated at the base, giving the necessary conditions of identifiability. Application to an I4 mechanism is achieved with experimental results.

**Index Terms**—Calibration, computer vision, legs observation, parallel mechanisms.

## I. INTRODUCTION

**A**MONG the proposed architectures for parallel mechanisms, structures with linear actuators at the base are of great interest: inertial effects are lowered, and the use of modern linear actuators enables one to build mechanisms with high dynamics. Consequently, many recently developed structures belong to this class of mechanisms such as Hexaglide [2], I4 [1], and Orthoglide [3]. Their use is highly dependent on their accuracy. Compared to serial mechanisms, they may exhibit a much better repeatability [4], but not necessarily a better accuracy, because of their large numbers of links and passive joints [5]. A kinematic calibration is thus needed for these structures.

The different approaches proposed to perform the kinematic calibration of parallel mechanisms are based on the minimization of an error function which depends on a set of geometrical

parameters defining the mechanism. With error functions expressed using the direct kinematic model, similar to the calibration of open-loop mechanisms, numerical models have generally to be used, leading to stability and convergence problems in the identification process [6].

Kinematic constraints on the end-effector or on the kinematic chains connecting the base and the end-effector, also called the legs of the mechanism, can be used to obtain redundant information and achieve the calibration [7]–[9]. However, accurate constraints on large structures are difficult to obtain, and the induced workspace limitations during the calibration process lower the identification efficiency [10].

The inverse kinematic model can generally be derived analytically [4]. Kinematic parameters can therefore be obtained by comparing the joint encoder values to their estimation using the model and a pose measurement [11]. Vision enables one to perform such a calibration [12]. However, the calibration efficiency is limited for a large mechanism workspace, as the ratio between measurement accuracy and measurement volume lowers. Furthermore, the calibration procedure seems tedious to achieve online: the end-effector is generally inaccessible or its observation impossible because of the environment, with, for instance, lubricant projections in a machine tool.

The use of redundant proprioceptive sensors located in the passive joints of the legs [6], [7], [13]–[15] remedy the two previous drawbacks. No external device has to be added to perform the calibration, and the measurement accuracy is not bound to the mechanism workspace. Such an approach is also efficient because the end-effector behavior is closely bound to the description of the legs. For the Stewart–Gough platform, the inverse kinematic model Jacobian matrix is for instance composed of the Plücker coordinates of the legs [16]. The main drawback of this calibration method is the need to install the redundant proprioceptive sensors in the mechanism passive joints, which has to be planned in the mechanism design.

In this paper, we propose an original approach that combines the advantages of a method based on the use of an exteroceptive sensor and of a method based on redundant proprioceptive sensors: using a camera to observe the legs of the mechanism, one can determine from their image their pose with respect to the camera. This information is closely linked to the mechanism kinematics, such as with a calibration method based on redundant proprioceptive sensors. Legs can be observed more easily than the end-effector, so that online identification may be achieved. At the same time, the use of a camera does not imply any mechanism modification, and the measurement system may be easily installed. The parallel mechanisms considered in this paper are actuated with linear actuators at the base.

Manuscript received August 1, 2003; revised January 6, 2004 and June 14, 2004. This paper was recommended for publication by Associate Editor H. Zhuang and Editor I. Walker upon evaluation of the reviewers' comments. This work was supported in part by CPER Auvergne 2001–2003 and by the CNRS-ROBEA Program through the MAX Project.

P. Renaud was with Laboratoire de Recherches et Applications en Mécanique Avancée (LaRAMA), Institut Français de Mécanique Avancée (IFMA), Université Blaise Pascal, 63175 Aubiere, France, and LASMEA, CNRS, Université Blaise Pascal, 63177 Aubiere, France. He is now with the LICIA, INSA Strasbourg, 67084 Strasbourg, France (e-mail: renaud.pierre@mail.insa-strasbourg.fr).

N. Andreff and P. Martinet are with the LASMEA, CNRS, Université Blaise Pascal, 63177 Aubiere, France (e-mail: andreff@lasmea.univ-bpclermont.fr; martinet@lasmea.univ-bpclermont.fr).

G. Gogu is with the Laboratoire de Mécanique et Ingénieries (LaMI), CNRS, Institut Français de Mécanique Avancée (IFMA), Université Blaise Pascal, 63175 Aubiere, France (e-mail: gogu@ifma.fr).

Digital Object Identifier 10.1109/TRO.2005.847606

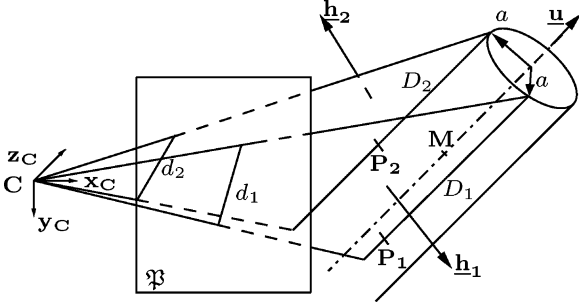


Fig. 1. Perspective projection of a cylinder and its outline in the sensor frame.

In Section II, the information that can be obtained by observation of the legs of the mechanism is outlined. In Section III, the mechanism modeling considered during the calibration is presented, before giving the proposed calibration method in Section IV. Experimental results obtained on an I4 mechanism are then introduced, before presenting concluding remarks on the approach and its further developments.

## II. MEASURE FROM THE IMAGE

The kinematic chains connecting the base and the end-effector are often composed of cylindrical elements, because of their stiffness and their availability as standard industrial components. We hence consider in the following that such elements can be observed. In this section, the relationship that can be expressed between the position and orientation of cylindrical elements of known radius  $a$  (see the notations in the Appendix) and their image is outlined in order to make the paper self-contained.

### A. Camera Behavior

The image formation is assumed to be modeled by the pinhole model [17], [18], and the camera is first calibrated [19]. Optical distortions can then be indeed compensated so that they are not considered explicitly in the following expressions, and, for the sake of clarity, a unit focal length is considered.

### B. From Image to Pose Estimation

Due to the perspective projection, a cylinder image is composed of two lines (Fig. 1), generally intersecting except if the cylinder axis is going through the camera center of projection  $C$ . We assume that these two lines can be extracted from the images [20]. Each cylinder generating line  $D_i$ ,  $i \in [1, 2]$ , corresponding to one line  $d_i$  in the image can be defined by its Plücker coordinates [21]  $(\underline{u}, \underline{h}_i)$  where  $\underline{u}$  is the unit vector of the cylinder axis and  $\underline{h}_i$  is defined by

$$\underline{h}_i = \underline{u} \times \underline{CP}_i \quad \forall i \in [1, 2] \quad (1)$$

where  $\underline{P}_i$  is an arbitrary point of  $D_i$  and  $\times$  represents the vector cross product.

By definition,  $\underline{h}_i$  is perpendicular to any vector defined between  $C$  and a point of  $d_i$ . The equation of  $d_i$ ,  $i \in [1, 2]$ , in the image plane  $\mathfrak{P}$  is therefore expressed as  $(x \ y \ 1)^T \cdot \underline{h}_i = 0$  where  $\underline{h}_i = \underline{h}_i / \|\underline{h}_i\|$  and  $\cdot$  represents the scalar product. Consequently, one can immediately determine the vectors  $\underline{h}_i$ ,  $i \in [1, 2]$ , in the camera frame  $\{C\} = (C, \underline{x}_C, \underline{y}_C, \underline{z}_C)$  (Fig. 1).

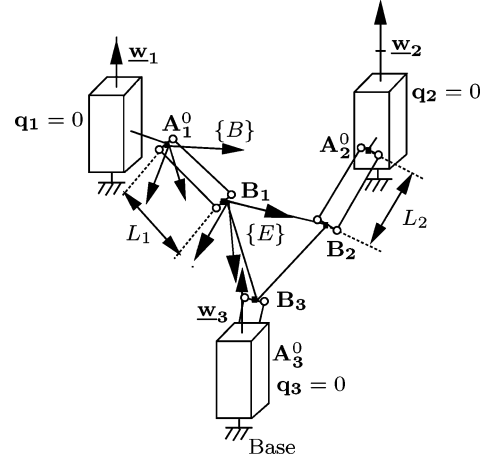


Fig. 2. Identifiable mechanism: the Delta mechanism with linear actuators at the base ( $n = 3$ ) [22].

The cylinder axis direction  $\underline{u}$  can therefore be computed from (1) by

$$\underline{u} = \frac{\underline{h}_1 \times \underline{h}_2}{\|\underline{h}_1 \times \underline{h}_2\|}. \quad (2)$$

The distances between the cylinder axis and the generating lines are equal to the cylinder radius  $a$ . Simple geometry allows one to check that the vectors  $\underline{h}_i$ ,  $i \in [1, 2]$ , are normal to the tangent planes to the cylinder. Hence, any point  $M$  belonging to the cylinder axis can therefore be found in the one-dimensional kernel of

$$\underline{h}_i \cdot M = \pm a, \quad i \in [1, 2]. \quad (3)$$

The determination of the sign of the right-hand side of (3) is performed in the grayscale image by analyzing the position of the cylinder with respect to the generating line.

From the observation of a cylindrical element with a camera, it is thus possible to determine the position and orientation of its axis in the camera frame. In Section IV, this information is used for the calibration. In Section III, we present first the mechanism modeling.

## III. MECHANISM KINEMATIC MODELING

### A. Mechanism Structure

We consider a parallel mechanism composed of a base, an end-effector, and  $n$  kinematic chains connecting them (Fig. 2—see notations in the Appendix). We consider each kinematic chain composed of two elements linked in  $\underline{A}_j$ ,  $j \in [1, n]$ . One element is linked to the base by means of an actuated prismatic joint. The other is linked to the end-effector in  $\underline{B}_j$ ,  $j \in [1, n]$ , with a spherical, revolute, or universal joint. The joint in  $\underline{A}_j$  may be a revolute, spherical, or universal joint. Articulated parallelograms are also considered as possible elements connected to the end-effector.

### B. Hypotheses

Wang and Masory [5] have shown that the influence of the joint defects on the mechanism accuracy is negligible compared to the influence of the joint positioning errors for a

Stewart–Gough platform. This result is considered to be valid in our context, due to the accuracy of the now available industrial components, so that the mechanism geometry is defined by the relative positions of the joint characteristic elements. For prismatic and revolute joints, these characteristic elements are their axis unit vector and the position of a point on the joint axis. A spherical joint is defined only by its center. A universal joint, which is composed of two perpendicular intersecting revolute joints, is defined by its center and one revolute joint axis.

The articulated parallelograms are considered to be perfect, which means that their sides stay parallel by pairs. They can then be defined for the calibration by equivalent links connecting the centers of the small parallelogram sides, of dimension equal to the parallelogram long side. For the sake of notation simplicity, the centers of the small parallelogram sides will be denominated as joint centers in the following.

The elements observed with the camera are those connected to the end-effector. The axes of the cylindrical elements and the lines joining the points  $\mathbf{A}_j$  and  $\mathbf{B}_j$ ,  $j \in [1, n]$ , are considered to be parallel.

### C. Kinematic Parameters

For universal or spherical joints, the points  $\mathbf{A}_j$  and  $\mathbf{B}_j$ ,  $j \in [1, n]$ , are the joint centers. For a revolute joint, they are defined as the intersection between the joint axis and the leg element axis.

The position of the joint centers  $\mathbf{A}_j$ ,  $j \in [1, n]$ , vary with the value of the linear actuator encoders. To describe them, we consider the position  $\mathbf{A}_j^0$  when the encoder value of the associated linear actuator is equal to zero. The mechanism is then described by the following kinematic parameters:

- the position of the joint centers between the leg elements  $\mathbf{A}_j^0$ ,  $j \in [1, n]$ ;
- the actuator axes  $\underline{\mathbf{w}}_j$ ,  $j \in [1, n]$ ;
- the axis directions  $\underline{\mathbf{v}}_j$  of the revolute and universal joints located in  $\mathbf{A}_j$ , if necessary;
- the lengths  $L_j$ ,  $j \in [1, n]$ , of the elements connected to the end-effector;
- the position of the joint centers on the end-effector  $\mathbf{B}_j$ ,  $j \in [1, n]$ , and, if necessary, the axis directions of the revolute and universal joints on the end-effector.

### D. Defining the Reference Frames

Because of the relative displacements of the legs and the potential self-occlusions, the calibration method has to be elaborated considering that it is necessary to use several camera locations to observe all of the legs while the end-effector pose varies in the workspace. Several camera frames will be defined accordingly, so that we identify directly the kinematic parameters in frames which are intrinsically defined from the mechanism joints.

- For a spatial mechanism, the frame  $\{B\}$  associated with the base can be defined from three distinct joint centers  $\mathbf{A}_j^0$  and the end-effector frame  $\{E\}$  defined from three distinct joint centers  $\mathbf{B}_j$ . In Fig. 2, the frame definitions are illustrated for  $n = 3$  legs. If  $n > 3$ , the frames are

TABLE I  
CALIBRATION METHOD STRUCTURE

<b>Step 1</b>	Base parameter estimation in the camera frames $\rightarrow (\mathbf{A}_j^0, \underline{\mathbf{v}}_j, \underline{\mathbf{w}}_j)_{C_\alpha}$
<b>Step 2</b>	Parameter estimation in the base frame $\rightarrow (\mathbf{A}_j^0, \underline{\mathbf{v}}_j, \underline{\mathbf{w}}_j)_B$
<b>Step 3</b>	Estimation of the length of the elements connected to the end-effector $\rightarrow L_j$
<b>Step 4</b>	Parameter estimation in the end-effector frame $\rightarrow (\mathbf{B}_j, \underline{\mathbf{v}}_j)_E$

defined from three distinct joint centers selected among the  $n$  joint centers.

- For a planar mechanism, the joints in  $\mathbf{A}_j$  and the prismatic joints on the base are defined by their relative positions and the rotation axis perpendicular to the mechanism plane. The base frame  $\{B\}$  can then be defined by this axis and the position of two joint centers  $\mathbf{A}_j^0$ . The definition of  $\{E\}$  requires then only two joint centers as the mechanism plane is already defined with the base frame.

## IV. CALIBRATION METHOD

To identify the kinematic parameters described in the former section, we propose a calibration method using a camera to observe the cylindrical elements connected to the end-effector.

To ensure the observability of the legs, the camera is supposed to be located in  $N_C$  successive locations (see the notations in Table V). No assumption is done on these locations or on the corresponding end-effector poses. The camera relative positions are indeed not considered to be known accurately and the end-effector poses can be different for each camera position. The method is composed of four steps (Table I). The first one is performed to obtain information in the camera frames and the kinematic parameters are determined in the three following steps. It must be outlined that steps 2 and 3 are actually independent, which tends to minimize the error propagation in the calibration process.

### A. Step 1—Base Parameter Estimation in the Camera Frames

In the first step, the characteristic elements of the joints on the base are identified, as well as those defining the joints between the two elements composing a leg. Let  $\{C_\alpha\}$  be the  $\alpha$ th camera frame,  $\alpha \in [1, N_C]$ . The parameters associated with one leg are determined in two stages.

1) *Stage 1*: In the first stage, the end-effector is moved to modify the leg orientation, while locking the corresponding actuator in a position  $m$  (Fig. 3). The observation of leg  $j$  in  $N_I$  different orientations enables one to compute the  $j$ th joint center  $\mathbf{A}_j^m$  and the joint axis  $\underline{\mathbf{v}}_j$ :

- Joint center—The joint located at  $\mathbf{A}_j$  belongs to the leg axis, which can be expressed by

$$\mathbf{A}_j^m \mathbf{M}_{j,k} \times \underline{\mathbf{u}}_{j,k} = 0, \quad k \in [1, N_I] \quad (4)$$

where  $\underline{\mathbf{u}}_{j,k}$  and  $\mathbf{M}_{j,k}$  are known from Section II. The coordinates of  $\mathbf{A}_j^m$  in the camera frame can therefore be computed by solving the overdetermined linear system obtained by concatenation of the  $3N_I$  vector equations (4). As the three equations provided by the cross product for

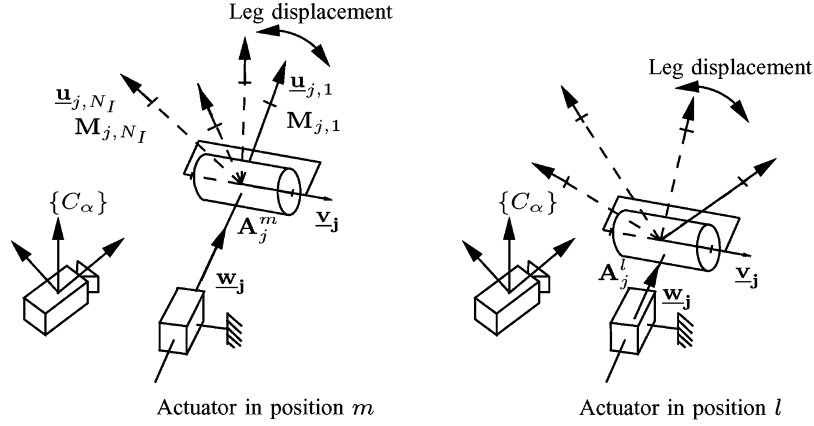


Fig. 3. Step 1—Determination of the actuator axis and the characteristic elements of the joint between the leg elements in two stages. Example of a revolute joint.

each pose are not independent, the solution is obtained by a singular value decomposition. It can be easily proved that two leg orientations are at least necessary to estimate the joint center position:  $N_I \geq 2$

- Joint axis—For a revolute joint, the joint axis unit vector  $\underline{v}_j$  is perpendicular to the leg axis for the  $N_I$  end-effector poses

$$\underline{v}_j \cdot \underline{u}_{j,k} = 0, \quad k \in [1, N_I]. \quad (5)$$

The vector  $\underline{v}_j$  can hence be determined by solving the overdetermined linear system obtained from the  $N_I$  equations (5). Here again, two different leg orientations are necessary to estimate the vector.

For a universal joint, if the revolute joint axis orientations have an influence on the mechanism kinematics, they will be estimated in the fourth step.

2) *Stage 2:* In the second stage, the joint center  $\mathbf{A}_j$  is displaced using the corresponding actuator to a new position  $\mathbf{A}_j^l$ . The actuator encoder gives us the value of the displacement  $\mathbf{q}_j^l - \mathbf{q}_j^m$  between the two positions  $m$  and  $l$ . By repeating the first stage procedure for the new joint center position  $\mathbf{A}_j^l$ , the prismatic joint unit axis can then be easily determined from

$$\mathbf{A}_j^m \mathbf{A}_j^l = (\mathbf{q}_j^l - \mathbf{q}_j^m) \underline{w}_j. \quad (6)$$

In the previous equation, the only unknown term in the camera frame is the vector  $\underline{w}_j$ . Using at least four leg images, the characteristic elements of the prismatic joint and the joint located between the leg elements can finally be estimated in the camera frame. One may notice that it is possible then to express the joint center  $\mathbf{A}_j$  position in the camera frame for any actuator position and in particular for the actuator encoder zero value  $\mathbf{A}_j^0$ .

### B. Step 2—Parameter Estimation in the Base Frame

1) *Principle:* At the end of the first step, the characteristic elements of some joints located in  $\mathbf{A}_j$ ,  $j \in [1, n]$ , or on the base are determined in different camera frames  $\{C_\alpha\}$ . Expressing these elements in the base frame requires the knowledge of the  $N_C$  successive camera poses with respect to the base. Designing a system to impose accurately the different camera locations would be expensive and its use restricting, so that the different camera poses with respect to the base are computed. This com-

putation can be achieved explicitly, introducing the  $6N_C$  corresponding unknowns, or implicitly by directly searching the kinematic parameters in the base frame. The latter solution is selected since it enables one to keep the number of parameters to identify independent from the number of camera locations. Furthermore, the need of *a priori* knowledge of the homogeneous transformations  ${}^B T_{C_\alpha}$  between the base and the camera frames is suppressed, which is of great interest as the camera frames are not physically measurable. To determine the kinematic parameters in the base frame, an error function is expressed using the invariance of the scalar product with Euclidian transformation. Scalar products are expressed both in the base frame and in the successive camera frames.

2) *Error Function:* For a given camera frame  $\{C_\alpha\}$ ,  $n_\alpha$  legs are considered observable for any end-effector pose. Let  $r_\alpha$  be the revolute joint number among the joints of center  $\mathbf{A}_j$ .  $N_\alpha$  and  $R_\alpha$  are, respectively, the set of observable legs and the set of observable legs for the camera position  $\{C_\alpha\}$  with revolute joints in  $\mathbf{A}_j$ .

The position of the joint centers  $\mathbf{A}_j$ ,  $j \in [1, n]$ , when the actuator encoder values are equal to zero are estimated in the first step in the camera frames, as well as the actuator axes and the revolute joint axes. From the  $n_\alpha$  positions  $\mathbf{A}_j^0$ ,  $j \in N_\alpha$ ,  $(n_\alpha - 1)$  independent vectors  $\mathbf{A}_j^0 \mathbf{A}_g^0$ ,  $(j, g) \in N_\alpha$ , can be computed. The actuator axes  $\underline{w}_j$ ,  $j \in N_\alpha$ , and revolute joint axes  $\underline{v}_j$ ,  $j \in R_\alpha$  are also known in the camera frames. One can then constitute a vector set  $\mathbf{V}$  of independent vectors

$$\mathbf{V} = \{\mathbf{A}_j^0 \mathbf{A}_g^0, (j, g) \in N_\alpha\} \cup \{\underline{v}_j, j \in R_\alpha\} \cup \{\underline{w}_j, j \in N_\alpha\} \quad \forall \alpha \in [1, N_C]. \quad (7)$$

Consequently the kinematic parameters in the base frame  $\{B\}$  are determined by nonlinear minimization of the error function  $F_1$

$$F_1 \left( \{\mathbf{A}_j^0, \underline{v}_j, \underline{w}_j\}_{j \in [1, n]} \right) = \sum_{\alpha=1}^{N_C} \sum_{(p,q)} [\mathbf{V}_p \cdot \mathbf{V}_q|_{C_\alpha} - \mathbf{V}_p \cdot \mathbf{V}_q|_B]^2 \quad (8)$$

where  $N_C$  is the number of successive camera frames and  $\mathbf{V}_p$  and  $\mathbf{V}_q$  are two elements of  $\mathbf{V}$  and  $*|_R$  representing the frame  $\{R\}$  used to express the terms of  $\mathbf{V}$ .

3) *Identifiability*: Two necessary conditions must be fulfilled to identify the kinematic parameters in the base frame.

- 1) Each leg of the mechanism has to be observed for at least one camera position to ensure that the corresponding kinematic parameters are included in  $F_1$ .
- 2) The number of independent equations contained in  $F_1$  has to be greater or equal to the number of kinematic parameters. For a spatial mechanism, three parameters are necessary to define the relative positions of the joints used to define the base frame. Three parameters are necessary for each additional joint center and two parameters for a revolute joint axis or actuator axis. The number  $n_b$  of parameters to identify is then equal to

$$n_b = 3 + 3(n - 3) + 2r + 2n = 5n + 2r - 6 \quad (9)$$

where  $n$  is the number of legs and  $r$  is the number of legs with revolute joints in  $\mathbf{A}_j$ .

For a planar mechanism, two parameters are necessary to define the relative positions of the joint centers used to define the base frame as well as the vector perpendicular to the mechanism plane. Any additional joint only requires two parameters for its center and one parameter for an actuator axis. The revolute joint axes are perpendicular to the mechanism plane so that the number  $n_b$  of parameters to identify is equal to

$$n_b = 2 + 2(n - 2) + n = 3n - 2. \quad (10)$$

From the elements of  $\mathbf{V}$ ,  $C_{n_\alpha}^2 = n_\alpha(n_\alpha - 1)/2$  independent scalar products can be expressed between the vectors  $\mathbf{A}_j^0 \mathbf{A}_g^0$ ,  $(j, g) \in N_\alpha$ ,  $j \geq g$ . It is also possible to compute  $C_{r_\alpha}^2$  scalar products between the vectors  $\underline{\mathbf{v}}_j$ ,  $j \in R_\alpha$ , and  $C_{n_\alpha}^2$  products between the actuator axes  $\underline{\mathbf{w}}_j$ ,  $j \in N_\alpha$ . Considering also the scalar products between the three types of vectors, the second necessary identifiability condition can be expressed by

$$\sum_{\alpha=1}^{N_C} (2C_{n_\alpha}^2 + C_{r_\alpha}^2 + (r_\alpha + n_\alpha)(n_\alpha - 1) + n_\alpha r_\alpha) \geq n_b. \quad (11)$$

The two identifiability conditions are necessary to perform the identification. Their sufficiency depends on the movements of the legs, which is specific to the mechanism.

At the end of this second step, all of the kinematic parameters related to the actuators and the joints between the leg elements, except those describing the revolute joint axes, are identified in the base frame.

### C. Step 3—Identification of the Length of the Elements Connected to the End-Effector

1) *Principle*: At the end of the first step, one can express the position of the joint center  $\mathbf{A}_j$  between the two leg elements for any end-effector pose. The position of the joint center  $\mathbf{B}_j$  can hence be written as a function of the length of the element connected to the end-effector

$$\mathbf{B}_{j,k}|_{C_\alpha} = \mathbf{A}_{j,k}|_{C_\alpha} + L_j \underline{\mathbf{u}}_{j,k}|_{C_\alpha}, \quad k \in [1, N_I] \quad (12)$$

where  $\mathbf{B}_{j,k}$  (respectively  $\mathbf{A}_{j,k}$ ) the position of  $\mathbf{B}_j$  ( $\mathbf{A}_j$ ) for the  $k$ th end-effector pose and  $\underline{\mathbf{u}}_{j,k}$  the unit axis vector of the ob-

served element, determined from its image. An error function is introduced by considering like Notash [23] the invariance of the distances between the joint centers on the end-effector.

2) *Error Function*: The invariance of the distance between two joint centers  $\mathbf{B}_j$  and  $\mathbf{B}_g$  can be expressed by

$$\|\mathbf{B}_{j,k+1} \mathbf{B}_{g,k+1}\|_{C_\alpha} = \|\mathbf{B}_{j,k} \mathbf{B}_{g,k}\|_{C_\alpha}, \quad k \in [1, N_I - 1] \quad (13)$$

using (12) to compute the vectors  $\|\mathbf{B}_j \mathbf{B}_g\|$ . The lengths  $L_j$ ,  $j \in [1, n]$ , of the elements connected to the end-effector are therefore determined by nonlinear minimization of the error function  $F_2$

$$F_2(L_j) = \sum_{\alpha=1}^{N_C} \sum_{k=1}^{N_I-1} \sum_{\substack{(j,g) \in N_\alpha \\ g > j}} [\|\mathbf{B}_{j,k+1} \mathbf{B}_{g,k+1}\|_{C_\alpha}^2 - \|\mathbf{B}_{j,k} \mathbf{B}_{g,k}\|_{C_\alpha}^2]^2. \quad (14)$$

3) *Identifiability*: The estimation of the lengths  $L_j$ ,  $j \in [1, n]$ , is possible if, first, all of the legs are observed at least once with the successive camera locations, which is already a necessary condition in the second step. The number of independent equations contained in  $F_2$  also has to be greater or equal to the number  $n$  of lengths to identify

$$\sum_{\alpha=1}^{N_C} C_{n_\alpha}^2 \geq n. \quad (15)$$

At the end of the third step, all of the lengths of the elements connected to the end-effector are identified. It is important to note that this step is independent from the previous one. No error propagation hence occurs.

### D. Step 4—Parameter Estimation in the End-Effector Frame

In the fourth step, all of the parameters related to the joints on the end-effector are identified. The axes of the universal joints located between the leg elements are also identified if necessary.

1) *Joint Centers*: The previous step enables one to determine the values of the distances  $\|\mathbf{B}_j \mathbf{B}_g\|$ . The relative positions of the joint centers  $\mathbf{B}_j$ ,  $j \in [1, n]$ , are therefore estimated by expressing the distance invariance with Euclidian transformation and finally minimizing the error function  $F_3$

$$F_3(\mathbf{B}_j|_E) = \sum_{\alpha=1}^{N_C} \sum_{\substack{(j,g) \in N_\alpha \\ g > j}} [ \|\mathbf{B}_j \mathbf{B}_g\|_{C_\alpha}^2 - \|\mathbf{B}_j \mathbf{B}_g\|_E^2 ]^2. \quad (16)$$

To do so, each leg has to be observed at least once with the camera, which constitutes the first identifiability condition. The number of equations contained in (16) also has to be greater than or equal to the number of parameters needed to define the joint center  $\mathbf{B}_j$ ,  $j \in [1, n]$ , positions in the end-effector frame. For a spatial mechanism, three parameters are necessary to define the positions of the three joint centers used to define the end-effector frame. Three parameters are also needed for each joint center remaining, so that the number  $n_e$  of parameters to identify is equal to

$$n_e = 3 + 3(n - 3) = 3n - 6. \quad (17)$$

For a planar mechanism, as the plane has already been defined with the joints on the base, only one parameter is needed to define the relative positions of the joints defining the end-effector frame, and two parameters are needed for any other joint, so that the number  $n_e$  is then equal to

$$n_e = 1 + 2(n - 2) = 2n - 3. \quad (18)$$

The second identifiability condition is then

$$\sum_{\alpha=1}^{N_C} C_{n_\alpha}^2 \geq n_e. \quad (19)$$

2) *Revolute Joint Axes*: The position of the joint centers  $\mathbf{B}_j, j \in [1, n]$ , is then known in the end-effector frame  $\{E\}$  and in some camera frames  $\{C_\alpha\}, \alpha \in [1, N_C]$ . The homogeneous transformation  ${}^{C_\alpha}T_E = ({}^{C_\alpha}\mathbf{R}_E, {}^{C_\alpha}\mathbf{t}_E)$  between each frame  $\{C_\alpha\}$  and  $\{E\}$  can hence be estimated by expressing the coordinates of  $\mathbf{B}_j$  in the camera frames as a function of the transformation

$$({}^{C_\alpha}\mathbf{R}_E \mathbf{B}_j|_E + {}^{C_\alpha}\mathbf{t}_E) \times \mathbf{B}_{j,k}|_{C_\alpha} = 0 \quad \forall k \in [1, N_I]. \quad (20)$$

The relation (20) provides us with two independent equations for one end-effector pose and for one observed leg. Three legs are thus needed to compute the six parameters defining the transformation  ${}^{C_\alpha}T_E$  as

$$n_\alpha \geq 3. \quad (21)$$

From  ${}^{C_\alpha}T_E$ , it is then possible to express the legs orientations  $\mathbf{u}_{j,k}, k \in [1, N_I]$ , and the position of the axes points  $\mathbf{M}_{j,k}, k \in [1, N_I]$ , in the end-effector frame. The determination of the revolute joint axes is then similar to the one achieved in the first step. Two leg orientations are needed. For a planar mechanism, this computation is not needed as the revolute joint axes are determined in the second step.

3) *Universal Joint Axes*: After the first and second steps, the joint centers  $\mathbf{A}_j$  are expressed in the base frame  $\{B\}$  and in the camera frames  $\{C_\alpha\}$ . The computation of the transformation  ${}^{C_\alpha}T_B$  is therefore similar to the determination of  ${}^{C_\alpha}T_E$  achieved in the previous paragraph, using the relation

$$({}^{C_\alpha}\mathbf{R}_B \mathbf{A}_j|_B + {}^{C_\alpha}\mathbf{t}_B) \times \mathbf{A}_{j,k}|_{C_\alpha} = 0, \quad \forall k \in [1, N_I]. \quad (22)$$

Three legs have to be observed simultaneously. In such a case, the knowledge of  ${}^{C_\alpha}T_B$  and  ${}^{C_\alpha}T_E$  allows one to compute  ${}^B T_E$  and identify the universal joint axes with an error function based on the inverse kinematic model.

### E. Extension of the Method

The calibration method presented here allows one to identify the kinematic parameters defining mechanisms with legs connecting the base and the end-effector. For some mechanisms like the I4 [1], the element on which the legs are connected is articulated. The calibration method can easily be adapted, as we will demonstrate in the next section, by modifying the error functions to take into account the mobility of the elements.

One may notice that the method has been presented assuming that one camera is placed in  $N_C$  different locations. Several

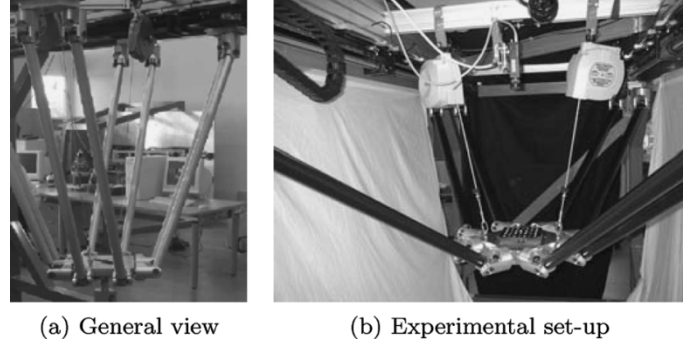


Fig. 4. I4 mechanism—general view and experimental setup.

cameras may be used to reduce the experimental procedure. The number  $N_C$  represents then the total number of locations of the different cameras.

## V. APPLICATION—THE I4 MECHANISM

### A. Mechanism Structure

The I4 mechanism [1] is a 4-DOF mechanism actuated by four linear actuators fixed on the base [Fig. 4(a)]. Four legs, constituted by articulated parallelograms, link the actuators to a traveling plate which itself supports the end-effector. The parallelograms are articulated with spherical joints. Since these parallelograms are designed to be identical, the traveling plate displacements are only composed of translations, and the parallelogram sides stay parallel by pairs. The end-effector can be translated in three directions, and rotated by the relative displacement of the two plate parts [Fig. 5(b)], using two rack-and-pinion systems.

Contrary to the description of the mechanism performed in Section III, the element connected to the legs of the mechanism is not the end-effector. This induces some slight modifications of the parameterization and the calibration method that will be presented. Moreover, modeling is also modified to take into account the manufacturing tolerances.

### B. Modeling

1) *Hypotheses*: As mentioned in Section II, the articulated parallelograms are modeled by equivalent elements of same length linked in  $\mathbf{A}_j, i \in [1, 4]$  and  $\mathbf{B}_j, j \in [1, 4]$  [Fig. 5(a)].

Because of the manufacturing tolerances, some assumptions that were made during the design of the mechanism are considered to be valid for the calibration: the actuator axes are considered parallel and coplanar, as well as the points  $\mathbf{A}_j, j \in [1, 4]$ , and located on two lines [Fig. 5(a)]. The four parallelograms are considered to be identical with a length  $L$ .

2) *Parameterization*: The base frame  $\{B\}(\mathbf{O}, \mathbf{x}_B, \mathbf{y}_B, \mathbf{z}_B)$  is defined using as the frame origin the joint center  $\mathbf{A}_1$  position when the corresponding actuator encoder value is equal to zero. The four points  $\mathbf{A}_j, j \in [1, 4]$  are located in the  $(\mathbf{x}_B, \mathbf{y}_B)$  plane and  $\mathbf{A}_1 \mathbf{A}_2$  parallel to the  $\mathbf{x}_B$  axis.

The end-effector is connected to the traveling plate elements with a revolute joint and two rack-and-pinion systems. There-

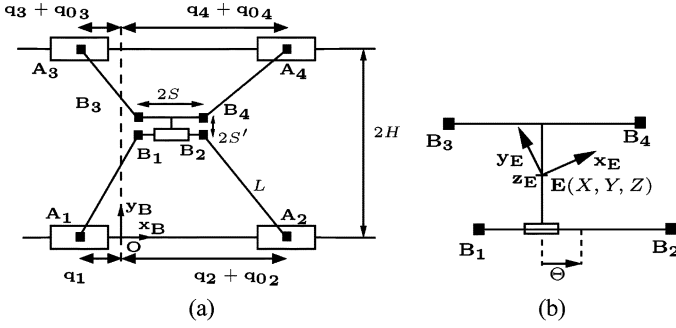


Fig. 5. I4 mechanism geometry. (a) Mechanism. (b) Traveling plate.

fore, the end-effector frame  $\{E\}(\mathbf{E}, \mathbf{x}_E, \mathbf{y}_E, \mathbf{z}_E)$  cannot be described using the joints between the end-effector and the legs, as proposed in Section II. Here, the origin of the end-effector frame is defined as the intersection between the axis of the revolute joints and the plane containing the points  $\mathbf{B}_j$ ,  $j \in [1, 4]$  [Fig. 5(b)]. The orientation of the vectors  $\mathbf{x}_E$  and  $\mathbf{y}_E$  is selected to be the same as  $\mathbf{x}_B$  and  $\mathbf{y}_B$  when the lines  $\mathbf{B}_1\mathbf{B}_3$  and  $\mathbf{B}_2\mathbf{B}_4$  are parallel to  $\mathbf{y}_B$ . The end-effector pose is defined by the position  $(X, Y, Z)$  of the end-effector frame origin and its orientation  $\Theta$  with respect to the base frame.

3) *Kinematic Parameters*: Because of the design assumptions, the number of parameters needed to define the location of the joint centers  $\mathbf{A}_j$ ,  $j \in [1, 4]$ , and the actuator axes is reduced compared to the modeling presented in Section II. Four parameters are needed: the distance  $2H$  between the two actuator axes and three encoder offsets  $\mathbf{q}_{0j}$ ,  $j \in [2, 4]$ , so that

$$\mathbf{A}_1^0 \mathbf{A}_i \cdot \mathbf{x}_B = \mathbf{q}_i + \mathbf{q}_{0i}. \quad (23)$$

The relative position of the joint centers  $\mathbf{B}_j$ ,  $j \in [1, 4]$ , is defined by the dimensions  $S$  and  $S'$ . One parameter  $L$  expresses the parallelogram length. Seven parameters finally define the mechanism geometry:  $(H, \mathbf{q}_{02}, \mathbf{q}_{03}, \mathbf{q}_{04}, S, S', \text{ and } L)$ .

### C. Calibration Method

The calibration method presented in Section III is applied to the I4 mechanism. First, it should be noticed that, due to the mechanism geometry, it is possible to observe the four legs simultaneously (Fig. 6) with one camera position:  $N_C = 1$  in the following. Second, some slight modifications are needed to take into account the existence of the traveling plate between the legs and the end-effector as follows.

1) *Step 1*: The end-effector is displaced while sequentially locking the actuators. For each locked actuator, the position of the corresponding spherical joints that compose the articulated parallelograms can therefore be determined in the camera frame (Fig. 7). From each couple of spherical joints, one can then compute the joint center  $\mathbf{A}_j$ ,  $j \in [1, 4]$ , in the camera frame. As points  $\mathbf{A}_1$  and  $\mathbf{A}_2$  are aligned with the actuator axes, as well as  $\mathbf{A}_3$  and  $\mathbf{A}_4$ , only the first stage of step 1 is needed for each joint to determine the actuator axis  $\mathbf{x}_B$  in the camera frame. The position of the points  $\mathbf{A}_j$ ,  $j \in [1, 4]$ , for the actuator zero encoder value can hence be also determined. One may notice that the unit vector  $\mathbf{z}_B$  perpendicular to the plane containing the joint centers can be computed at the same time, and consequently the unit vector  $\mathbf{y}_B$  also.

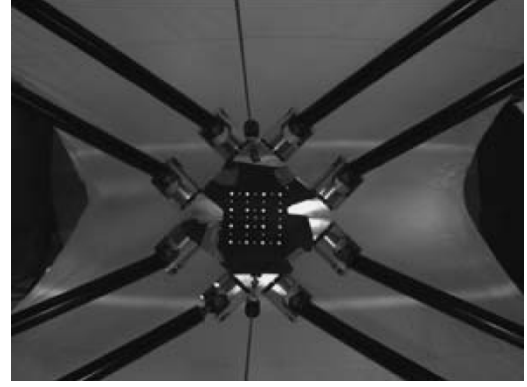


Fig. 6. Leg image with the camera.

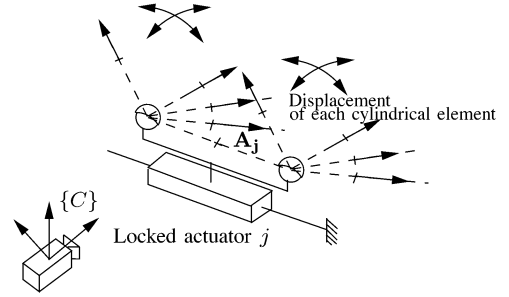


Fig. 7. Identification of the joint centers in the camera frame.

2) *Step 2*: The joint centers  $\mathbf{A}_j$ ,  $j \in [1, 4]$ , are defined in the base frame by four parameters:  $(\mathbf{q}_{02}, \mathbf{q}_{03}, \mathbf{q}_{04}, \text{ and } H)$ . Due to the mechanical design, the actuator axes are parallel to the vectors  $\mathbf{A}_1\mathbf{A}_2$  and  $\mathbf{A}_3\mathbf{A}_4$ . No kinematic parameter is then necessary to define them. The vector set  $\mathbf{V}$  (7) is then reduced to

$$\mathbf{V} = (\mathbf{A}_1^0 \mathbf{A}_2^0, \mathbf{A}_1^0 \mathbf{A}_3^0, \mathbf{A}_1^0 \mathbf{A}_4^0) \quad (24)$$

with

$$\begin{cases} \mathbf{A}_1^0 \mathbf{A}_2^0 = \mathbf{q}_{02} \mathbf{x}_B \\ \mathbf{A}_1^0 \mathbf{A}_3^0 = \mathbf{q}_{03} \mathbf{x}_B + 2H \mathbf{y}_B \\ \mathbf{A}_1^0 \mathbf{A}_4^0 = \mathbf{q}_{04} \mathbf{x}_B + 2H \mathbf{y}_B. \end{cases}$$

Six independent equations can be expressed from the elements of  $\mathbf{V}$ , which ensures the identifiability of the four kinematic parameters.

3) *Step 3*: Only the distances  $\|\mathbf{B}_1\mathbf{B}_2\|$  and  $\|\mathbf{B}_3\mathbf{B}_4\|$  are invariant with an end-effector pose modification. Therefore, the error function  $F_2(L)$  just takes into account these two distances. Two independent pieces of information can be obtained, so that the identifiability of the parameter  $L$  is ensured.

4) *Step 4*: The use of the error function introduced in the third section is simplified here because of the mechanism design. The distances  $\|\mathbf{B}_1\mathbf{B}_2\|$  and  $\|\mathbf{B}_3\mathbf{B}_4\|$  included in the error function  $F_3$  are only depending on the parameter  $S$ , which is therefore immediately determined. To determine the other dimension  $S'$ , the relative displacement of the two traveling plate elements has to be taken into account. The distance between  $\mathbf{B}_1$  (respectively  $\mathbf{B}_3$ ) and  $\mathbf{B}_2$  ( $\mathbf{B}_4$ ) along  $\mathbf{y}_B$  is constant and known in the camera frame, with, for instance

$$\mathbf{B}_1\mathbf{B}_3 \cdot \mathbf{y}_B = -L \underline{\mathbf{u}}_{1,k} \cdot \mathbf{y}_B + 2(H - S') + L \underline{\mathbf{u}}_{3,k} \cdot \mathbf{y}_B \quad \forall k. \quad (25)$$

TABLE II  
A PRIORI AND IDENTIFIED KINEMATIC PARAMETERS

Parameter	$L$	$H$	$S$	$S'$
<i>A priori</i>	1.0010m	0.5000m	0.1536m	0.1536m
Identified	1.0213m	0.4985m	0.1598m	0.1602m
Parameter	$\mathbf{q}_2$	$\mathbf{q}_3$	$\mathbf{q}_4$	
<i>A priori</i>	1.5705m	1.2190m	2.8700m	
Identified	1.5675m	1.2190m	2.7867m	

The corresponding distance  $2S'$  is hence also immediately identified.

#### D. Experimental Setup

A  $1024 \times 768$  CCD camera with a 3.6-mm lens is located on the base of the mechanism so that the four legs are observable, as well as a calibration board linked to the end-effector [Figs. 4(b) and 6]. The calibration board is composed of 16 white dots that enables one by their observation to perform end-effector pose measurements to evaluate the calibration efficiency. Five poses are considered for each joint location determination in step 1). Another 20-pose set is used for steps 2)–4).

#### E. Experimental Results

The accuracy of the determination of the spherical joint centers in step 1) can be estimated from the residuals of (4). For this experiment, the joint centers location is determined with an accuracy of the order of 1 mm, which is probably due to the errors in the compensation of the optical distortions and the limited resolution of the camera sensor. The kinematic parameters identified in the other three steps are indicated in Table II with the *a priori* values. The parameter value modifications are noticeable, with variations of the order of several millimeters.

The calibration board linked to the end-effector can be used to evaluate the accuracy improvement using the identified parameters. Its observation enables us to measure its pose with respect to the camera. The end-effector displacement between two poses can therefore be estimated from these poses measurements. On the other hand, the end-effector displacement can be estimated using the direct kinematic model, the proprioceptive sensor values recorded during the experiment and a kinematic parameter set, either identified or estimated *a priori*. If the estimated displacements are equal to the real ones, the gaps between the measurements and the estimated displacements are equal to the measurement noise, which has been previously evaluated to be zero-mean with standard deviation in the order of 0.2 mm. The average value of the gaps for a set of measurements should then tend to be equal to zero, and the standard deviation equal to the standard deviation of the measurement noise. For the 20-pose set used during the calibration, the average value is reduced from  $-63$  to  $-3.4 \mu\text{m}$  and the standard deviation of the errors is reduced from 0.53 to 0.33 mm. The gap between estimated displacements and vision-based displacement measurements is hence lowered significantly using the identified kinematic parameters.

TABLE III  
NOTATIONS RELATED TO THE IMAGE FORMATION

$\mathbf{C}$	Camera center of projection
$D_i, i \in [1, 2]$	Cylinder outline lines
$d_i$	The image of the line $D_i$
$\mathbf{u}$	The unit vector of the cylinder axis
$\mathbf{M}$	A point belonging to the cylinder axis
$(\mathbf{h}_1, \mathbf{h}_2)$	Unit vectors perpendicular to the planes containing the cylinder generating lines and $\mathbf{C}$
$a$	The cylinder radius
$\{\mathbf{C}\}(\mathbf{C}, \mathbf{x}_C, \mathbf{y}_C, \mathbf{z}_C)$	The camera frame

TABLE IV  
NOTATIONS RELATED TO THE GEOMETRY OF THE MECHANISM

$n$	The number of legs
$\mathbf{A}_j$	The center of the joint between the two elements of the leg $j$ ( $j \in [1, n]$ )
$\mathbf{A}_j^0$	The position of the joint center when the encoder value of the corresponding actuator is equal to zero: $\mathbf{q}_j = 0$
$\mathbf{w}_j$	The unit vector of the $j$ -th linear actuator axis
$\mathbf{v}_j$	The unit vector of the axis of the $j^{\text{th}}$ revolute or universal joint
$L_j$	The length of the element of the leg $j$ connected to the end-effector
$\mathbf{B}_j$	The center of the joint of leg $j$ on the end-effector
$\{\mathbf{B}\}$	The base frame
$\{\mathbf{E}\}$	The end-effector frame

## VI. CONCLUSION

Parallel mechanisms with linear actuators at the base are of great interest for applications where high dynamics are required. Like serial mechanisms, they need a kinematic calibration to improve their accuracy. In this paper, we proposed an original approach to achieve the calibration process by observing the legs with a camera. The ease of use and the absence of mechanism modifications due to the use of an exteroceptive sensor are combined with the advantage of having information directly bound to the mechanism kinematics, similar to methods based on the use of redundant proprioceptive sensors. The associated method has been developed from a theoretical point of view, giving identifiability necessary conditions as a function of the mechanism geometry. An evaluation has been then performed on an I4 mechanism, with a noticeable accuracy improvement according to vision-based pose measurement. Further developments concern first the calibration robustness to the measurement noise, with an influence analysis of the number of poses. Besides, the accuracy of the leg measurements is intrinsically bound to their pose with respect to the camera. The calibration efficiency will hence also be improved by an optimal selection of the poses for calibration and the camera locations with respect to the mechanism base. The optimization of this offline calibration process will then lead to the dynamic and online calibration of the mechanisms, which will necessitate taking into account the possible inertial effects.



TABLE V  
NOTATIONS RELATED TO THE CALIBRATION PROCEDURE

$N_C$	The number of successive camera locations used during the calibration
$\{C_\alpha\}$	The $\alpha$ -th camera frame, $\alpha \in [1, N_C]$
$N_I$	The number of images taken for one camera position
$A_{j,k}, k \in [1, N_I]$	The $N_I$ successive positions of the joint center $A_j$
$A_j^m$	The position of the joint center $A_j$ when the corresponding actuator is in position $m$
$q_j^m$	The value of the $j$ -th actuator encoder for the position $m$ of the actuator
$M_{j,k}, k \in [1, N_I]$	The $N_I$ successive positions of $M_j$ , a point belonging to the axis of the observed element cylinder $j$
$\underline{u}_{j,k}, k \in [1, N_I]$	The $N_I$ successive unit vectors of the axis of the observed element cylinder $j$
$n_\alpha$	The number of legs observed for the $\alpha$ -th position of the camera
$r_\alpha$	The number of legs observed for the $\alpha$ -th position of the camera frame with a revolute joint of center $A_j$
$N_\alpha(R_\alpha)$	The set of legs observed for the $\alpha$ -th position (with a revolute joint of center $A_j$ ) If for instance the legs (1, 3, 5) are observed, $n_\alpha = 3$ and $N_\alpha = \{1, 3, 5\}$
$r$	The number of legs with revolute joint of center $A_j, j \in [1, n]$
$C_p^q$	The binomial coefficient such that $C_p^q = \frac{p!}{q!(p-q)!}$
$n_e$	The number of parameters needed to define the end-effector frame $\{E\}$
$n_b$	The number of parameters needed to define the base frame $\{B\}$
$A_{j,k}, k \in [1, N_I]$	The $N_I$ successive positions of $A_j$ when displacing the end-effector

## APPENDIX

See the notations provided in Tables III–V.

## ACKNOWLEDGMENT

The authors would like to thank F. Pierrot and S. Krut, LIRMM, Montpellier, France, for their help and comments on the experiments.

## REFERENCES

- [1] S. Krut, O. Company, M. Benoit, H. Ota, and F. Pierrot, "I4: a new parallel mechanism for Scara motions," in *Proc. 2003 Int. Conf. Robotics and Automation*, Taipei, Taiwan, Sep. 2003, pp. 1875–1880.
- [2] M. Honegger, A. Codourey, and E. Burdet, "Adaptive control of the hexaglide, a 6 dof parallel manipulator," in *Proc. 1997 IEEE Int. Conf. Robotics and Automation*, Albuquerque, NM, Apr. 1997, pp. 543–548.
- [3] D. Chablat and P. Wenger, "Architecture optimization of a 3-DOF parallel mechanism for machining applications, the Orthoglide," *IEEE Trans. Robot. Automat.*, vol. 19, no. 3, pp. 403–410, Jun. 2003.
- [4] J.-P. Merlet, *Parallel Robots*. Norwell, MA: Kluwer, 2000.
- [5] J. Wang and O. Masory, "On the accuracy of a Stewart platform—part I: the effect of manufacturing tolerances," in *Proc. IEEE Int. Conf. Robotics and Automation*, Atlanta, GA, 1993, pp. 114–120.
- [6] D. Daney, "Étalonnage géométrique des robots parallèles," Ph.D. dissertation, Université de Nice-Sophia Antipolis, 2000.
- [7] W. Khalil and D. Murareci, "Autonomous calibration of parallel robots," in *Proc. 5th IFAC Symp. Robot Control*, Nantes, France, 1997, pp. 425–428.
- [8] W. Khalil and S. Besnard, "Self calibration of Stewart-Gough parallel robots without extra sensors," *IEEE Trans. Robot. Autom.*, vol. 15, no. 6, pp. 1116–1121, Dec. 1999.

- [9] D. Daney, "Self calibration of Gough platform using leg mobility constraints," in *Proc. 10th World Congress Theory of Machine and Mechanisms*, Oulu, Finland, 1999, pp. 104–109.
- [10] S. Besnard and W. Khalil, "Identifiable parameters for parallel robots kinematic calibration," in *Proc. IEEE Int. Conf. Robotics and Automation*, Seoul, Korea, 2001, pp. 2859–2866.
- [11] H. Zhuang, J. Yan, and O. Masory, "Calibration of Stewart platforms and other parallel manipulators by minimizing inverse kinematic residuals," *J. Robot. Syst.*, vol. 15, no. 7, pp. 395–405, 1998.
- [12] P. Renaud, N. Andreff, F. Marquet, and P. Martinet, "Vision-based kinematic calibration of a H4 parallel mechanism," in *Proc. IEEE Int. Conf. Robotics and Automation*, Taipei, Taiwan, Sep. 2003, pp. 1191–1196.
- [13] C. Wampler and T. Arai, "Calibration of robots having kinematic closed loops using nonlinear least-squares estimation," in *Proc. IFTOMM World Congress Mechanism and Machine Science*, Nagoya, Japan, Sep. 1992, pp. 153–158.
- [14] H. Zhuang, "Self-calibration of parallel mechanisms with a case study on Stewart platforms," *IEEE Trans. Robot. Autom.*, vol. 13, no. 3, pp. 387–397, Jun. 1997.
- [15] H. Zhuang and L. Liu, "Self calibration of a class of parallel manipulators," in *Proc. IEEE Int. Conf. Robotics and Automation*, Minneapolis, MN, 1996, pp. 994–999.
- [16] J.-P. Merlet, *Parallel Manipulators. Part 2—Singular Configurations and Grassmann Geometry*, INRIA, 1988.
- [17] O. Faugeras, *Three-Dimensional Computer Vision: A Geometric Viewpoint*. Cambridge, MA: MIT Press, 1993.
- [18] H. Zhuang and Z. Roth, *Camera-Aided Robot Calibration*. Boca Raton, FL: CRC Press, 1996.
- [19] J. Lavest and M. Dhôme, "Comment calibrer des objectifs très courte focale," in *Actes de Reconnaissance des Formes et Intelligence Artificielle (RFIA2000)*, Paris, France, 2000, pp. 81–90.
- [20] P. Renaud, N. Andreff, G. Gogu, and P. Martinet, "On vision-based kinematic calibration of a Stewart-Gough platform," in *Proc. 11th IFTOMM World Congress Mechanism and Machine Science*, Tianjin, China, Apr. 2004, pp. 1906–1911.
- [21] H. Pottmann, M. Peternell, and B. Ravani, "Approximation in line space—Applications in robot kinematics and surface reconstruction," in *Adv. Robot Kinemat.* Strobl, 1998, pp. 403–412.
- [22] P. Zobel, P. D. Stefano, and T. Raparelli, "The design of a 3 dof parallel robot with pneumatic drives," in *Proc. 27th Int. Symp. Industrial Robots*, Milan, Italy, Oct. 1996, pp. 707–710.
- [23] L. Notash and R. Podhorodeski, "Fixtureless calibration of parallel manipulators," *Trans. CSME*, vol. 21, no. 3, pp. 273–294, 1997.



medical robotics.



of modeling, identification, and control of mechanisms using computer vision.

**Pierre Renaud** received the Ph.D. degree in mechanical engineering from the Blaise Pascal University, Aubiere, France, in 2003.

From 2000 to 2003, he performed research at Institut Français de Mécanique Avancée (IFMA), Clermont-Ferrand, France, as an Assistant Lecturer. After a postdoctoral position at LIRMM, Montpellier, France, he is now an Associate Professor with INSA Strasbourg, Strasbourg, France. His current research interests are in the field of identification of parallel mechanisms using computer vision and

**Nicolas Andreff** graduated from the ENSEEIHT, Toulouse, France, and received the Ph.D. degree in computer graphics, computer vision and robotics from Institut National Polytechnique de Grenoble, Grenoble, France, in 1999.

From 1996 to 2000, he performed research at the Institut National de Recherche en Informatique et Automatique, Grenoble. Since 2000, he has been an Associate Professor with the Institut Français de Mécanique Avancée (IFMA), Clermont-Ferrand, France. His current research interests are in the field



**Philippe Martinet** graduated from the CUST, Clermont-Ferrand, France, in 1985 and received the Ph.D. degree in electronics science from the Blaise Pascal University, Clermont-Ferrand, France, in 1987.

Since 2000, he has been a Professor with Institut Français de Mécanique Avancée (IFMA), Clermont-Ferrand. He is performing research at the Robotics and Vision Group of LASMEA-CNRS, Clermont-Ferrand. His research interests include visual servoing, vision-based control, robust control, automatic guided vehicles, active vision and sensor

integration, visual tracking, and parallel architecture for visual servoing applications.



**Grigore Gogu** graduated as an Engineer from Brasov University, Brasov, Romania, where he received the Ph.D. degree in robotics.

He is now a Professor with Institut Français de Mécanique Avancée, Clermont-Ferrand, France. He is performing research at the Laboratoire de Mécanique et Ingénieries (LaMI), Aubiere, France. His current research interests include modeling, structural synthesis, and optimization of mechanisms and robots, dynamics of high-speed machine tools, methodology of innovation, and integrated design

and manufacturing.